

# Expression profiles of tRNA-derived fragments in high glucose-treated tubular epithelial cells

JIALING JI, JU RONG, HUI ZHENG, HUIMIN SHI, GAOTING QU,  
SHANWEN LI, WEIHUA GAN and AIQING ZHANG

Department of Pediatric Nephrology, The Second Affiliated Hospital of Nanjing Medical University,  
Nanjing, Jiangsu 210003, P.R. China

Received July 8, 2022; Accepted October 28, 2022

DOI: 10.3892/etm.2022.11725

**Abstract.** Transfer RNA-derived fragments (tRFs), a novel class of small non-coding RNA produced by the cleavage of pre- and mature tRNAs, are involved in various diseases. Renal tubulointerstitial fibrosis is a common final pathway in diabetic nephropathy (DN) in which hyperglycemia-induced tubular extracellular matrix (ECM) accumulation serves a vital role. The present study aimed to detect and investigate the role of tRFs in the accumulation of tubular ECM. Differentially expressed tRFs were analysed with high-throughput sequencing in primary mouse tubular epithelial cells treated with high glucose (HG). The Gene Ontology (GO) was used to analyze the potential molecular functions of these differentially expressed tRFs, and the Kyoto Encyclopedia of Genes and Genomes (KEGG) were used to analyze the associated signaling pathways involved in these differentially expressed tRFs. tRF-1:30-Gln-CTG-4 was overexpressed using tRF-1:30-Gln-CTG-4 mimic, followed by HG treatment. A total of 554 distinct tRFs were detected and 64 differentially expressed tRFs (fold change >2; P<0.05) were identified in tubular epithelial cells following high glucose (HG) treatment, among which 27 were upregulated and 37 were downregulated. Ten selected tRFs with the greatest difference (fold change >2; P<0.05) were verified to be consistent with small RNA-sequencing data, of which tRF-1:30-Gln-CTG-4 showed the most pronounced difference in expression and was significantly decreased in response to HG. GO analysis indicated that the differentially expressed tRFs were associated with 'cellular process', 'biological regulation' and 'metabolic process'. An analysis of the KEGG

database suggested that these differentially expressed tRFs were involved in 'autophagy' and signaling pathways for 'forkhead box O', 'the mammalian target of rapamycin' and 'mitogen-activated protein kinase'. Finally, the overexpression of tRF-1:30-Gln-CTG-4 ameliorated HG-induced ECM accumulation in tubular epithelial cells. Therefore, the present study demonstrated that there may be a significant association between tRFs and HG-induced ECM accumulation in tubular epithelial cells; these differentially expressed tRFs warrant further study to explore the pathogenesis of DN.

## Introduction

Diabetic nephropathy (DN), one of the most common and severe complications of diabetes mellitus, has developed in 40-50% of patients who are diabetic worldwide in the 2015-2020 and become the leading cause of end-stage renal disease (1,2), aggravating the global health and economic burden. Glomerulosclerosis, tubulointerstitial fibrosis (TIF) and chronic inflammation are characteristic pathological manifestations of DN (3). Increasing evidence indicates that renal TIF is the final common pathway and outcome of DN, accompanied by tubular atrophy and extracellular matrix (ECM) accumulation (4,5). However, the intrinsic mechanisms underlying TIF remain unclear. Thus, it is important to explore the mechanisms of TIF in DN.

Transfer RNA-derived fragments (tRFs), special types of small non-coding RNA (sncRNA), are more highly conserved than other sncRNAs and have attracted wide attention (6,7). tRFs are produced by specific cleavage of precursor or mature tRNA, and are classified into five subtypes: i) tRF-1; ii) tRF-2; iii) tRF-3; iv) tRF-5; and v) internal tRF (i-tRF) (8). Previous studies reported that tRFs can play crucial roles in biological processes in various types of disease, including neuronal degeneration, tumor cell proliferation and gene expression (9). Additionally, tRFs may participate in the early diagnosis of cancer by serving as prognostic biomarkers (10). A growing number of studies have demonstrated that tRFs may be associated with chronic kidney disease (CKD) progression (11-13). Khurana *et al* (11) identified that tRF<sup>Val</sup> and tRF<sup>Leu</sup>, derived from urinary exosomes, are suitable biomarkers for the early diagnosis of CKD. Our previous study also showed that tRFs contribute to podocyte differentiation to regulate CKD and

---

*Correspondence to:* Professor Aiqing Zhang or Professor Weihua Gan, Department of Pediatric Nephrology, The Second Affiliated Hospital of Nanjing Medical University, 262 Zhongshanbeitu, Nanjing, Jiangsu 210003, P.R. China  
E-mail: njaiqing@njmu.edu.cn  
E-mail: weihuagan@njmu.edu.cn

*Key words:* diabetic nephropathy, tubular epithelial cells, extracellular matrix, tRNA-derived fragment, tRF-1:30-Gln-CTG-4

revealed the potential mechanism of idiopathic nephrotic syndrome (12,13). To the best of our knowledge, however, little is known about the role of tRFs in TIF.

To explore the role of tRFs in TIF during DN progression, the present study performed high-throughput sequencing to detect differential expression profiles of tRFs in high glucose (HG)-treated tubular epithelial cells. Bioinformatics analyses were then conducted on these differentially regulated tRFs (fold change >2,  $P < 0.05$ ). The potential effect of specific tRF was investigated on HG-induced ECM accumulation of tubular epithelial cells. Therefore, the present study attempted to reveal the underlying mechanism of TIF from the novel perspective of tRFs and provide a promising therapeutic target for DN.

## Materials and methods

**Cell culture.** A total of 10 male 8-week-old C57BL/6 mice weighing 22-25 g (Vital River Laboratory Animal Technology Company; Beijing, China) were placed a standard environment on a 12-h light/dark cycle and suitable temperature (22-25°C) and humidity (40-70%) with free access to water and food. Primary mouse tubular epithelial cells were isolated from the renal cortex as previously described (14). All mice were euthanised by intraperitoneal injection of pentobarbital sodium (100 mg/kg) and the kidney was harvested. The cortical tissue was cut into 2-4 mm pieces and digested in 0.75 mg/ml collagenase for 1 h at 37°C. Subsequently, the digested tissues were filtered through 80- and 100-mesh steel sieves. Tubules in the 100-mesh steel sieve were collected and centrifuged at 3,000 x g for 20 min at 25°C. Finally,  $5 \times 10^6$  cells were suspended in Dulbecco's Modified Eagle Medium (DMEM) supplemented with 10% foetal bovine serum and 1% penicillin-streptomycin (all Gibco; Thermo Fisher Scientific, Inc.).  $2 \times 10^5$  cells (per well) were seeded into 12-well plates and treated with HG (35 mM) or normal glucose (control; 5 mM). D-mannitol (5 mM glucose + 30 mM D-mannitol) was used as the third group for balancing osmolality. Following 48 h HG treatment at 37°C, cells were harvested for subsequent experiments. The animal experiment was performed in accordance with Animal Research: Reporting of *In Vivo* Experiments guidelines (15), as well as the National Institutes of Health Guide for the Care and Use of Laboratory Animals (16), and was approved by the Institutional Animal Care and Use Committee of Nanjing Medical University (approval no. 2206034).

**Human serum samples.** Human serum samples from patients with DN were obtained from the Department of Endocrinology, The Second Affiliated Hospital of Nanjing Medical University, between 21 January 2021 and 17 September 2021. This study was approved by the Ethics Committee of Nanjing Medical University [approval no. (2022)-KY-037-01] and written informed consent was obtained from all patients. The information about the human subjects is summarized in Table SI.

**Immunofluorescence.** Cultured primary tubular epithelial cells were fixed with 4% paraformaldehyde for 15 min at room temperature and then incubated with primary antibody cytokeratin 18 (CK18; 1:200; cat. no. sc-32329; Santa Cruz Biotechnology, Inc.) at 4°C overnight. Subsequently, cells

were incubated with Alexa Fluor® 647-conjugated secondary antibody (goat anti-mouse IgG H&L; 1:400; cat. no. ab150115; Abcam) in the dark at room temperature for 2 h. After washing with phosphate-buffered saline, 0.02% DAPI staining was performed for 10 min at room temperature. Immuno-stained cells were observed under a fluorescence microscope (magnification, x100; Nikon Corporation).

**High-throughput sequencing.** High-throughput sequencing was performed as described previously (12). Briefly, total RNA samples were pretreated to remove RNA modifications that influence small RNA-sequencing (RNA-seq) library construction with the rtStar™ tRF&tiRNA Pretreatment kit (Arraystar, Inc.). The total RNA of each sample was sequentially ligated to 3' and 5' small RNA adapters. cDNA was synthesised and amplified using proprietary reverse transcription (RT) primers and amplification primers (NEBNext® Multiplex Small RNA Library Prep Set for Illumina; Illumina, Inc.). Subsequently, 134-160 bp PCR-amplified fragments were extracted and purified via 8% PAGE. Subsequently, completed libraries were quantified using the Agilent 2100 Bioanalyzer (Agilent Technologies, Inc.). The libraries were denatured and diluted to a loading volume of 1.3 ml and loading concentration of 1.8 pM following the manufacturer's protocol. Subsequently, according to the manufacturer's instructions, diluted libraries were loaded onto a reagent cartridge and forwarded to the sequencing run on Illumina NextSeq 500 system using NextSeq 500/550 V2 kit (cat. no. FC-404-2005; Illumina, Inc.).

**RNA extraction and RT-quantitative (q)PCR.** Total RNA was extracted from cells using TRIzol® reagent (Invitrogen; Thermo Fisher Scientific, Inc.) and RNA concentration and purity were detected using a NanoDrop instrument (Thermo Fisher Scientific, Inc.). RT-qPCR was performed using the HiScript III RT SuperMix and ChamQ™ SYBR® qPCR Master Mix (Vazyme Biotech Co., Ltd.) using the StepOne Real-Time PCR System (Applied Biosystems; Thermo Fisher Scientific, Inc.) according to the manufacturer's instructions. GAPDH was used as an internal control for normalisation. For expression of tRFs, total RNA samples were pretreated to remove RNA modifications with rtStar™ tRF&tiRNA Pretreatment kit (Arraystar, Inc.). PCR amplification was performed using the Bulge-Loop™ miRNA RT-qPCR Primer Sets (one RT primer and a pair of PCR primers for each set), which were designed specifically for each tRF by Guangzhou RiboBio Co., Ltd. After adding forward primer and universal reverse primer, the reaction mixtures were incubated at 95°C for 10 min, followed by 95°C for 2 sec, 60°C for 20 sec and 70°C for 10 sec, for 40 PCR cycles in the StepOne Real-Time PCR System (Applied Biosystems; Thermo Fisher Scientific, Inc.). U6 small nuclear RNA (snRNA) was used as the internal reference. All tRF primers were designed specifically by Guangzhou RiboBio Co., Ltd. and all mRNA primers were obtained from Genaray Biotech Co. Ltd. The mRNA and tRF forward primer sequences are listed in Tables SII and SIII. The Bulge-Loop™ U6 snRNA qPCR Primer Set (cat. no. MQP-0201) and universal reverse primer (cat. no. ssD089261711) cannot be provided due to the patent of Guangzhou RiboBio Co., Ltd. The relative expression levels were normalized to endogenous controls and were expressed as  $2^{-\Delta\Delta C_q}$  (17).

**Western blotting.** Western blotting was performed as described by Ji *et al* (18). Briefly, cells were harvested using RIPA Lysis Buffer supplemented with 1% protease inhibitor phenylmethylsulfonyl fluoride (both Beyotime Institute of Biotechnology). Total protein (25 ug) loaded per lane were separated by 10% SDS-PAGE and were transferred onto PVDF membranes (MilliporeSigma; cat. no. HATF09025). Then, membranes were blocked with 5% skimmed milk at room temperature for 2 h. Subsequently, membranes were incubated with primary antibodies against  $\alpha$ -smooth muscle actin ( $\alpha$ -SMA; 1:1,000; cat. no. BF9212; Affinity Biosciences, Ltd.), collagen I (1:1,000; cat. no. ab34710; Abcam), fibronectin (1:1,000; cat. no. ab2413; Abcam) and GAPDH (1:1,000; cat. no. AF7021; Affinity Biosciences, Ltd.) at 4°C overnight. Next day, membranes were washed using 1x TBST supplemented with 0.1% Tween 20, and then incubated with the secondary horseradish peroxidase (HRP)-conjugated antibodies (goat anti-mouse IgG; 1:2,000; cat. no. S002; Affinity Biosciences, Ltd; or goat anti-rabbit IgG; 1:2,000; cat. no. S001; Affinity Biosciences, Ltd.) at room temperature for 2 h. Finally, the membranes were incubated with ECL Developer (Biosharp) Intensity values expressed as relative protein expression were analysed using ImageJ software (version 1.8.0; National Institutes of Health) and normalised to the expression of GAPDH.

**Gene Ontology (GO) and pathway analysis.** To explore the potential functions of differentially expressed tRFs, target genes of differentially expressed tRFs (fold change >2 and  $P < 0.05$  for significantly differentially expressed tRFs) were selected. DAVID (david.ncifcrf.gov/) website was used for GO and Kyoto Encyclopedia of Genes and Genomes (KEGG; kegg.jp/) was used to perform pathway analysis.

**Transfection.** Mouse renal tubular epithelial cells were seeded in 12-well plates and grown to ~70% confluence ( $2 \times 10^5$  cells per well) at 37°C. The tRF-1:30-Gln-CTG-4 mimic (tRF mimic; 5'-GGTTCCATGGTGTAATGGTGAGCACTC TGG-3'; Guangzhou RiboBio Co., Ltd.) or negative control (NC mimic; 5'-UUUAUAGUCGUGGGAGCAGGAUCGGCU UCUNC-3'; Guangzhou RiboBio Co., Ltd.) were transfected into cells at a concentration of 30 nM with RiboFECT™ CP Transfection Reagent (Guangzhou RiboBio Co., Ltd.) for 6 h at 37°C according to the manufacturer's instructions. Then, the medium was replaced with complete DMEM and cells were stimulated with HG (35 mM) at 37°C for 48 h.

**Statistical analysis.** Data are expressed as the mean  $\pm$  standard error of the mean. All experiments were repeated three times. Statistical analyses were performed using Statistical Package for the Social Sciences version 22.0 (IBM Corp.). Student's t test was used for comparisons between two groups (unpaired). To compare >2 groups, one-way ANOVA followed by a Bonferroni's correction was used to analyse differences.  $P < 0.05$  was considered to indicate a statistically significant difference.

## Results

**tRF expression profiles in HG-treated tubular epithelial cells.** First, the purity of primary tubular epithelial cells was identified

using immunofluorescence staining with an epithelial-specific marker (CK18). The present results showed that >95% of cells expressed CK18 (Fig. S1). Subsequently, tubular epithelial cell ECM accumulation was induced by HG treatment. Meanwhile, D-mannitol was used to examine the effects of osmotic pressure on cells; osmotic pressure had no effect on the production of ECM in tubular epithelial cells (Fig. S2), which is consistent with previous studies (19,20). Thereafter, cells with a 5 mM glucose culture were selected as the control group. mRNA and protein expression of TIF-associated markers  $\alpha$ -SMA, collagen I and fibronectin (21,22) were significantly induced in the HG-treated group (Fig. 1A and B). Differentially expressed tRFs were analysed with high-throughput sequencing. Of 554 distinct tRFs detected, 64 differentially expressed tRFs (fold change >2;  $P < 0.05$ ) were identified. Of these, 27 tRFs were upregulated and 37 tRFs were downregulated, as displayed by hierarchical clustering heatmap and the volcano plot (Fig. 1C and D). All upregulated and downregulated tRFs in the two groups are listed in Table SIV. Commonly and specifically expressed tRFs are displayed in a Venn diagram (Fig. 1E). In total, 278 commonly expressed tRFs overlapped between the two groups, indicating non-zero counts per million mapped reads (CPM) values in both groups. In addition, 54 specifically expressed tRFs were found in the HG-treated group, whereas 27 specifically expressed tRFs were only detected in the control group. The tRF-5c, formed by cleavage at the D- and anticodon stems, was the most abundant tRF subtype in both the HG-treated and control groups, with expression in the HG-treated group higher than that in the control group (Fig. 1F and G), suggesting that tRF-5c may be associated with DN progression. Collectively, these results revealed that tRFs might play a role in HG-induced tubular ECM accumulation.

**Verification of expression levels of selected tRFs.** To verify the RNA-seq results, 10 tRFs with the greatest difference (fold change >2;  $P < 0.05$ ) were selected as candidate tRFs after excluding tRFs with zero CPM values. RT-qPCR analysis revealed that tRF-53:70-chrM.Trp-TCA, tRF-49:70-chrM.Trp-TCA, tRF-1:32-Glu-TTC-2 and tRF-1:32-Glu-TTC-1 were significantly upregulated in HG-treated tubular epithelial cells (Fig. 2B-E). tRF-1:30-Gln-CTG-4, tRF-1:28-Gly-CCC-1, tRF-1:29-Val-AAC-5 and tRF-1:30-Val-AAC-5 were significantly downregulated (Fig. 2F, G, I and J). However, there were no significant differences in the expression of tRF-1:32-Cys-GCA-1-M3 and tRF-1:29-Val-CAC-1 between the two groups (Fig. 2A and H). Among these verified tRFs, tRF-1:32-Glu-TTC-2, tRF-1:32-Glu-TTC-1, tRF-1:30-Gln-CTG-4, tRF-1:28-Gly-CCC-1, tRF-1:29-Val-AAC-5, tRF-1:32-Cys-GCA-1-M3, tRF-1:29-Val-CAC-1 and tRF-1:30-Val-AAC-5 belong to the tRF-5c subtype, tRF-53:70-chrM.Trp-TCA belongs to the tRF-3a subtype and tRF-49:70-chrM.Trp-TCA belongs to the tRF-3b subtype (Table SIV).

**GO and KEGG analysis of differentially expressed tRF targets.** tRFs may play a key role in post-transcriptional regulation via substantial tRF-target gene interactions (23). In the present study, target genes of the eight significantly differentially expressed tRFs were predicted to reveal potential underlying mechanisms of tRFs (Table SV). GO and KEGG

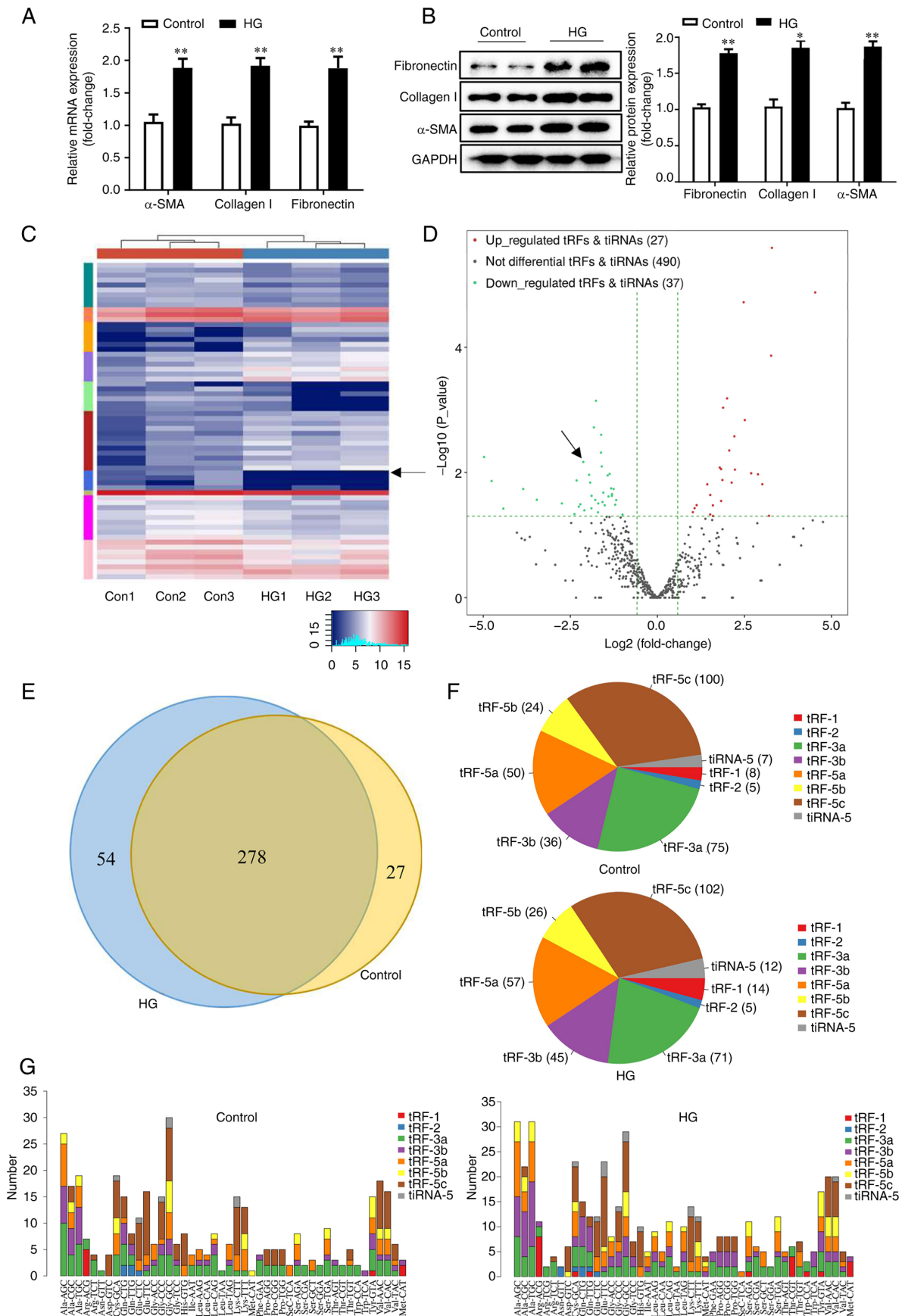


Figure 1. Identification of differentially regulated tRFs in HG-treated renal tubular epithelial cells. (A) mRNA and (B) protein expression levels of  $\alpha$ -SMA, collagen I and fibronectin. Relative levels were normalised to GAPDH. (C) Clustered heat map and (D) volcano plots of the differentially expressed tRFs in mouse renal tubular epithelial cells with or without HG treatment. Blue indicates a lower relative expression of tRFs. Red indicates a higher relative expression of tRFs. tRF indicated by the arrow is tRF-1:30-Gln-CTG-4. (E) tRFs that are commonly expressed in both groups and specifically expressed in one group. (F) The number of different types of tRFs in control and HG-treated groups. (G) The number of tRFs in different tRNAs in control and HG-treated groups. \* $P < 0.05$  and \*\* $P < 0.01$ . HG, high glucose; tRF, transfer RNA-derived fragment;  $\alpha$ -SMA,  $\alpha$ -smooth muscle actin.

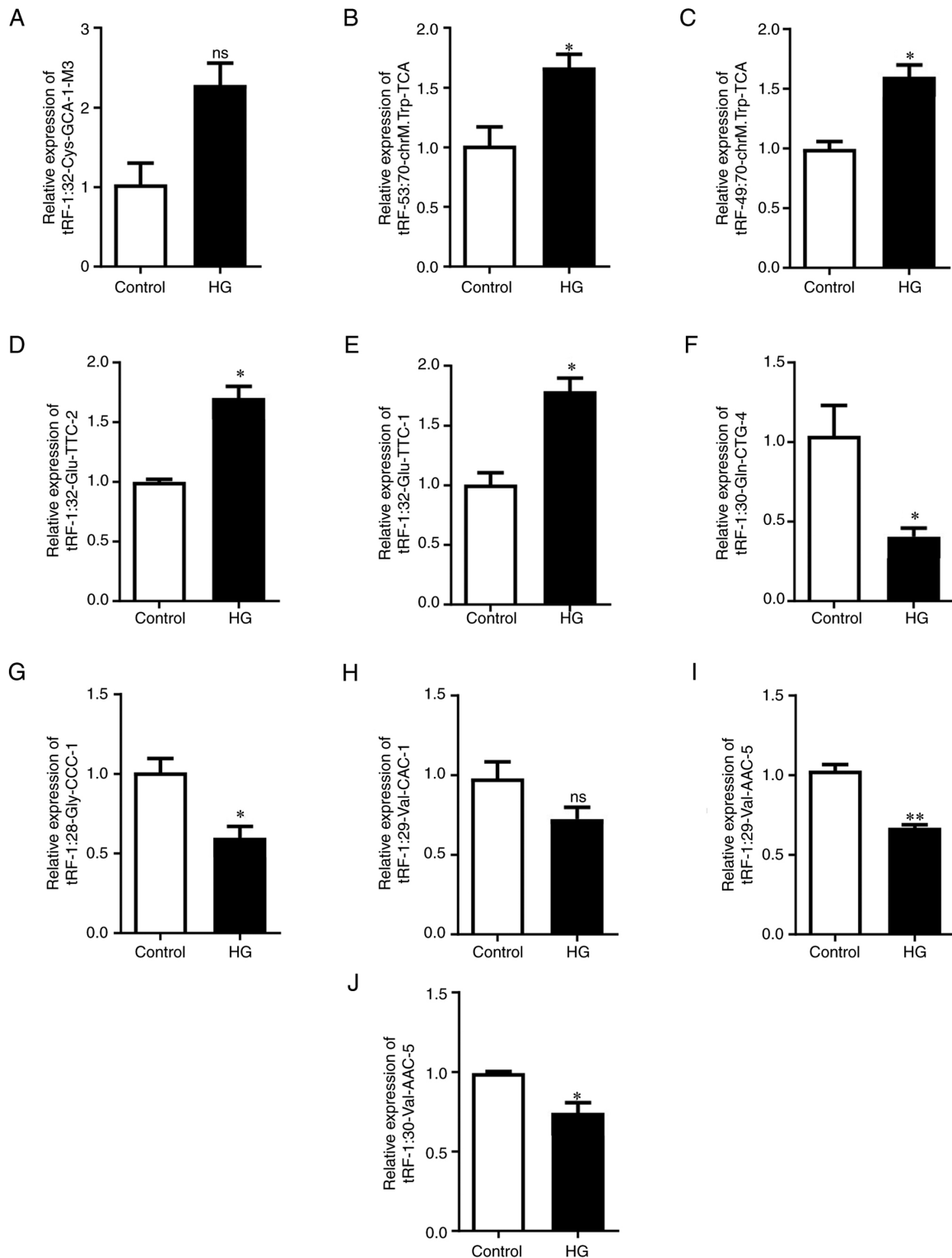


Figure 2. Verification of expression levels of selected tRFs by reverse transcription-quantitative PCR. Expression of (A) tRF-1:32-Cys-GCA-1-M3, (B) tRF-53:70-chrM.Trp-TCA, (C) tRF-49:70-chrM.Trp-TCA, (D) tRF-1:32-Glu-TTC-2, (E) tRF-1:32-Glu-TTC-1, (F) tRF-1:30-Gln-CTG-4, (G) tRF-1:28-Gly-CCC-1, (H) tRF-1:29-Val-CAC-1, (I) tRF-1:29-Val-AAC-5 and (J) tRF-1:30-Val-AAC-5. U6 was used as the internal reference for normalisation. \* $P < 0.05$  and \*\* $P < 0.01$ . ns, non-significant; tRF, transfer RNA-derived fragment.

analyses of these target genes evaluated the function of the differentially expressed tRFs. First, the potential function of downregulated tRF targets were assessed. The most highly enriched biological processes (BPs) were 'cellular process', 'biological regulation' and 'metabolic process' (Fig. 3A). 'Cellular anatomical entity', 'intracellular', 'organelle',

'cytoplasm' and 'membrane' were the most highly enriched cellular components (CCs; Fig. 3B). Molecular functions (MFs) primarily included 'protein binding', 'ion binding', 'organic cyclic compound binding', 'heterocyclic compound binding' and 'DNA binding' (Fig. 3C). The potential functions of upregulated tRF targets were consistent with those

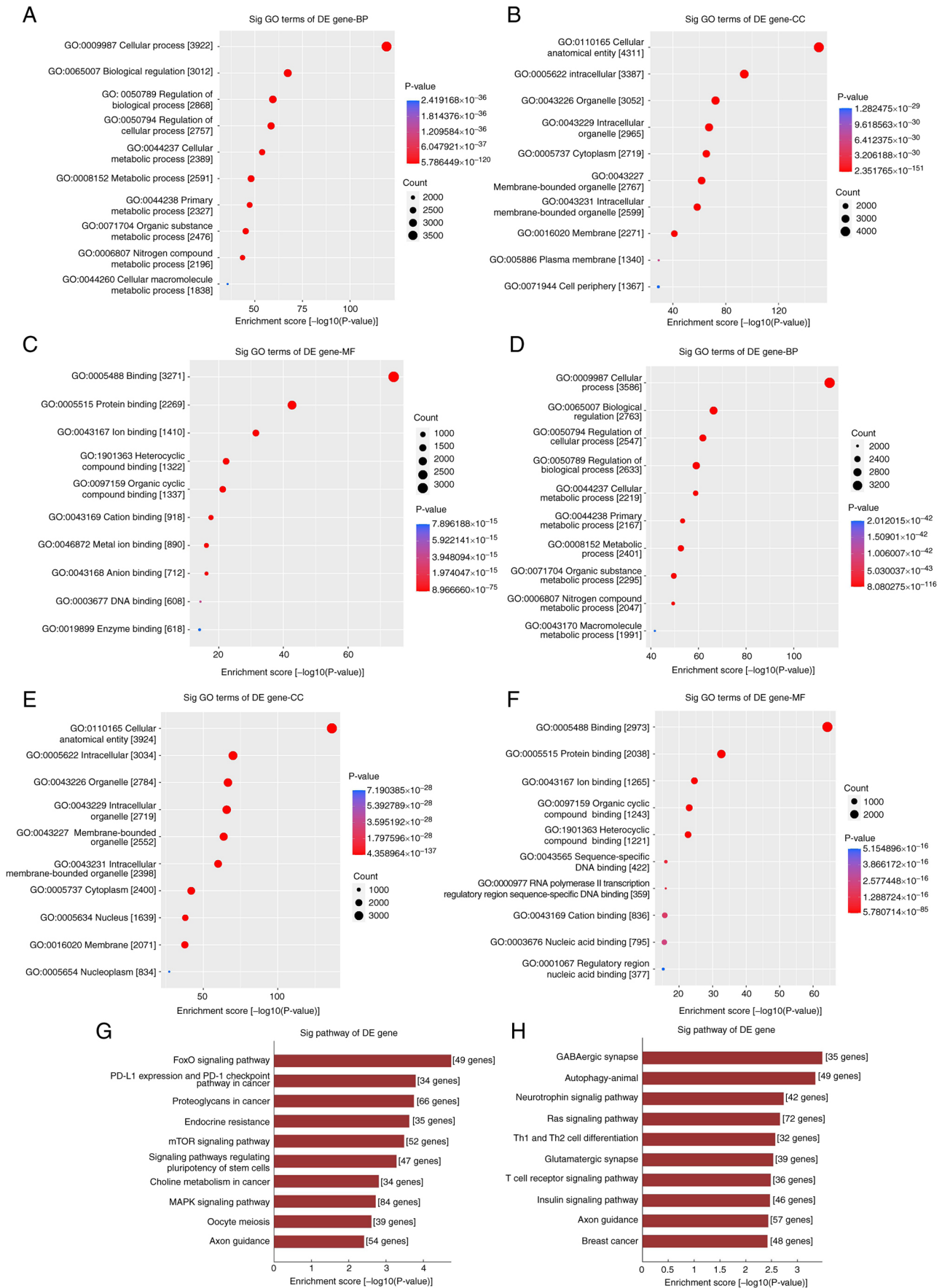


Figure 3. GO and KEGG analysis of potential genes of selected differentially downregulated and upregulated tRFs. GO analysis of the target genes of downregulated tRFs including (A) BP, (B) CC and (C) MF. GO analysis of the target genes of upregulated tRFs including (D) BP, (E) CC and (F) MF. (G) Analysis of potential target genes of selected differentially upregulated tRFs by KEGG pathway clustering. (H) KEGG pathway clustering analysis of potential target genes of the selected differentially downregulated tRFs. GO, Gene Ontology; KEGG, Kyoto Encyclopedia of Genes and Genomes; tRF, transfer RNA-derived fragment; BP, biological process; CC, cellular component; MF, molecular function; Sig, significant; DE, differentially expressed.

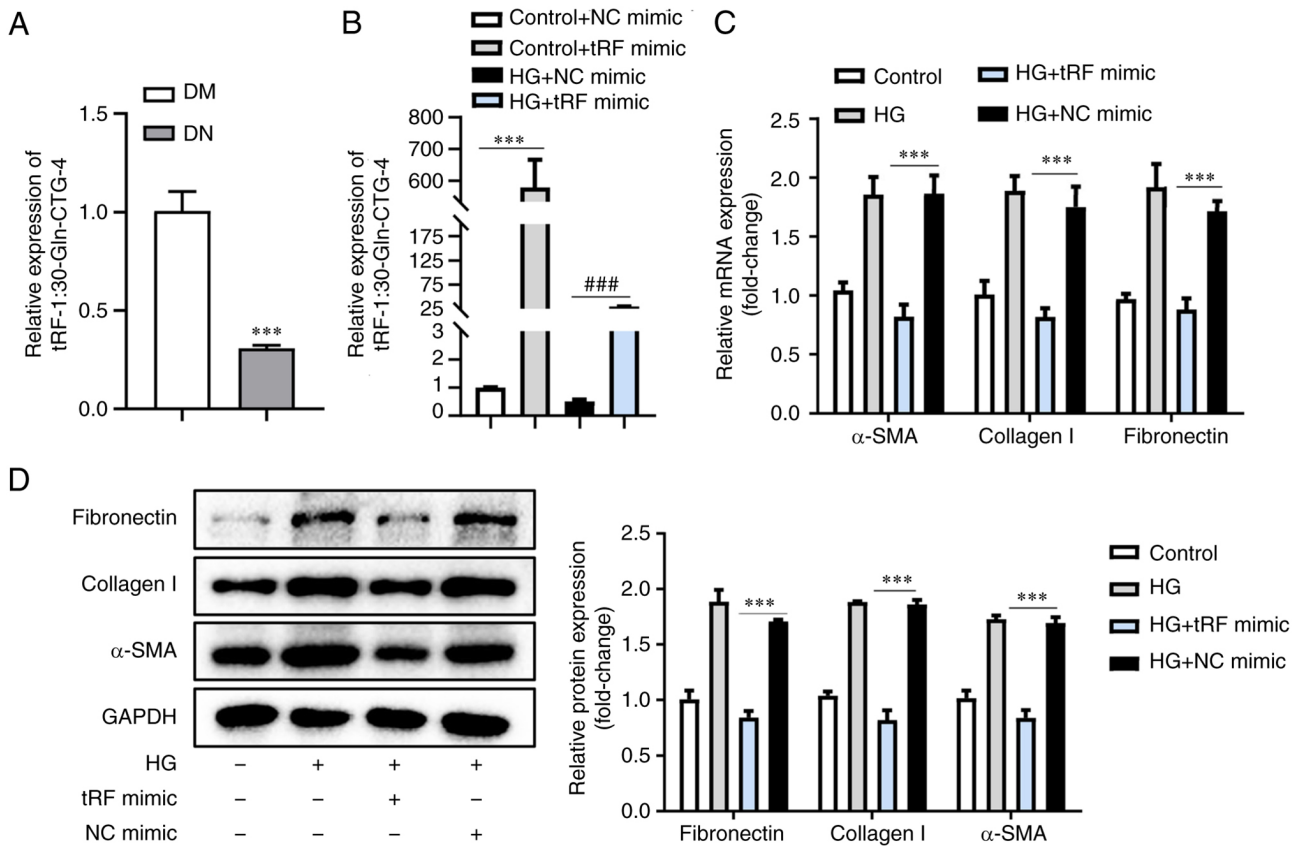


Figure 4. tRF-1:30-Gln-CTG-4 overexpression contributes to inhibition of extracellular matrix accumulation. (A) tRF-1:30-Gln-CTG-4 was validated by RT-qPCR, with U6 as a normalisation control. (B) RT-qPCR analysis of tRF-1:30-Gln-CTG-4 expression in mouse tubular epithelial cells transfected with tRF-1:30-Gln-CTG-4 mimic with or without HG treatment. (C) mRNA expression levels of  $\alpha$ -SMA, collagen-1 and fibronectin by RT-qPCR analysis. (D) Western blot analysis showing protein expression levels of  $\alpha$ -SMA, collagen-1 and fibronectin. The relative levels were normalised to those of GAPDH. \*\*\* $P$ <0.001 and ### $P$ <0.001. RT-qPCR, reverse transcription-quantitative PCR; tRF, transfer RNA-derived fragment;  $\alpha$ -SMA,  $\alpha$ -smooth muscle actin; HG, high glucose; DM, diabetes mellitus; DN, diabetic nephropathy; NC, negative control.

of downregulated tRF targets (Fig. 3D-F). In KEGG pathway enrichment analysis, forkhead box O ('FoxO signaling pathway'), 'PD-L1 expression and PD-1 checkpoint pathway in cancer', 'proteoglycans in cancer', 'endocrine resistance', 'mTOR signalling pathway' and 'MAPK signaling pathway' were highly enriched in the differentially upregulated tRFs (Fig. 3G). 'GABAergic synapse', 'autophagy-animal', 'neurotrophin signalling pathway', 'Ras signalling pathway', helper T ('Th1 and Th2 cell differentiation'), 'glutamatergic synapse', 'T cell receptor signalling pathway' and 'insulin signalling pathway' were highly enriched in the differentially downregulated tRFs (Fig. 3H).

**Overexpression of tRF-1:30-Gln-CTG-4 attenuates ECM deposition.** tRF-1:30-Gln-CTG-4 showed the most pronounced difference in expression and was significantly decreased in response to HG (Fig. 2). Moreover, tRF-1:30-Gln-CTG-4 expression in the serum of patients with DN was decreased by 30% (Fig. 4A). To explore the effects of tRF-1:30-Gln-CTG-4 on ECM deposition, tRF-1:30-Gln-CTG-4 was overexpressed using tRF-1:30-Gln-CTG-4 mimic, followed by HG treatment (Fig. 4B). There was a marked decrease in  $\alpha$ -SMA, collagen I and fibronectin levels (Fig. 4C and D), indicating an attenuated ECM deposition in tubular epithelial cells. These results demonstrated that tRF-1:30-Gln-CTG-4 was

involved in DN progression and may be a novel biomarker for DN progression.

## Discussion

Despite technological advances, the pathogenesis of DN remains unclear and, to the best of our knowledge, there are no valid therapeutic strategies (24,25). TIF is the key factor in DN progression, which is characterised by the deposition of ECM, including  $\alpha$ -SMA, fibronectin and collagen I (26). The present study found that tRFs, a special kind of sncRNA, are associated with TIF and involved in DN. These findings not only provide novel insights into the pathogenesis of DN but may also help to screen effective therapies for DN.

With advances in next-generation sequencing technology, numerous sncRNAs, including microRNAs, circular, p-element-induced wimpy testis-interacting and small nucleolar RNAs and tRNAs, have been confirmed to serve significant roles in a variety of diseases (27). Recently, tRNA-derived small fragments, called tsRNAs, have attracted considerable attention (28-30). The two types of tsRNA, tRNA-derived stress-induced RNA (tiRNA) and tRFs, are classified according to the different cleavage positions of the precursor or mature tRNA transcript (31). An increasing number of studies have demonstrated that tRFs serve a variety

of biological functions in regulating cell proliferation, interacting with proteins or mRNA and regulating the cell cycle, DNA damage response and epigenetic modifications (32-34). In addition, previous studies showed that tRFs may be novel diagnostic and therapeutic targets in kidney disease (11,35). Therefore, it was hypothesised that tRFs serve a key role in DN. To understand the potential effects of tRFs on DN, small RNA-seq was performed in the present study and 27 upregulated and 37 downregulated differentially expressed tRFs were found. These results suggest that tRFs may serve a crucial role in DN development and are worthy of further study.

To date, five types of tRFs have been identified and characterised by their provenance on tRNAs: tRF-1, tRF-2, tRF-3, tRF-5 and i-tRF. The tRF-1 subtype is derived from the 3' trailer of primary tRNA and is formed during the tRNA precursor sequence maturation. The tRF-2 subtype is derived from tRNA<sup>Glu</sup>, tRNA<sup>Gly</sup> and tRNA<sup>Tyr</sup>. The tRF-3 subtype that results from cleavage of the T-loop by the Dicer enzyme and ribonuclease angiogenin is further classified into two subgroups: tRF-3a; and tRF-3b. The tRF-5 subtype that is generated from the cleavage of the D-loop of tRNAs by the Dicer enzyme is further divided into three subtypes: tRF-5a, tRF-5b and tRF-5c. The i-tRF subtype originates from the internal bodies of mature tRNA (36-38). According to the present tRF high-throughput sequencing data, tRF-5c was the most abundant subtype in both the HG-treated and control groups. Furthermore, expression of tRF-5c in the HG-treated group was higher than that in the control group, suggesting that tRF-5c may be associated with DN progression.

Although there are some studies on the involvement of tRFs in pathogenesis of disease (39,40), to the best of our knowledge, the mechanisms by which tRFs regulate occurrence and development of diseases remain unclear. Previous studies have revealed that tRFs not only participate in posttranscriptional regulation via miRNA-like actions but also stabilise the mRNA by binding to RNA-binding proteins (41,42). For example, tRF3008A suppresses progression and metastasis of colorectal cancer by destabilising FOXP1 in an Argonaute protein-dependent manner (43). Goodarzi *et al* (44) showed that tRFs suppress breast cancer progression by competitively binding YBX1 to inhibit the stability of multiple oncogenic transcripts. Potential target genes of tRF-53:70-chrM.Trp-TCA, tRF-1:32-Glu-TTC-2, tRF-1:32-Glu-TTC-1, tRF-49:70-chrM.Trp-TCA, tRF-1:30-Gln-CTG-4, tRF-1:28-Gly-CCC-1, tRF-1:30-Val-AAC-5 and tRF-1:29-Val-AAC-5 were predicted in the present study. Analysis of tRF target genes revealed that multiple tRFs are associated with renal fibrosis. For example, tRF-1:28-Gly-CCC-1 is involved in regulating the fibrotic process by targeting transforming growth factor  $\beta$  receptor type 2, a type II serine/threonine kinase receptor for transforming growth factor  $\beta$ -1 (TGF- $\beta$ 1) that induces fibrosis by binding TGF- $\beta$ 1 and acting as the initiator and key component of canonical TGF- $\beta$ /SMAD signalling (45). tRF-1:30-Val-AAC-5 may function as an anti-fibrosis agent by targeting kelch-like protein 42 (KLHL42). Lear *et al* (46) showed that KLHL42 impairs TGF- $\beta$ -dependent profibrotic signalling and KLHL42 knockdown decreases fibrotic tissue production. In addition, in the present study FoxO3 was predicted as a target gene of tRF-1:30-Gln-CTG-4. Evidence has indicated that FoxO3 is an important player in fibrogenesis and a novel treatment strategy

in renal fibrosis (47). Hence, tRF-1:30-Gln-CTG-4 may serve a role in renal fibrosis by targeting FoxO3 expression. Further analysis of tRF target genes should be performed to explore the mechanisms of tRFs in TIF.

GO clustering was performed in the present study to investigate the potential functions of tRFs. For BP, most targets of differentially expressed tRFs were associated with cellular metabolic processes. In a pathology study of 34 cases of human kidneys diagnosed with DN, lipid accumulation was found in renal tubules (48). Moreover, *in vitro* studies showed lipid droplets in cultured renal tubular epithelial cells following HG treatment (49,50); these data demonstrate that tRF-associated metabolic disorders of renal epithelial cells may result in progressive fibrosis in DN. In addition, the most highly enriched MF subcategory in the present study was 'protein binding'. tRFs competitively bind RNA-binding proteins (RBPs) to regulate oncogenic mRNA expression. Falconi *et al* (51) indicated that a novel tRF derived from mature tRNA<sup>Glu</sup> was able to bind and displace the 3' untranslated region of specific RBPs to suppress breast cancer progression. The present GO analysis results provide novel ideas for exploring the role of tRFs in DN.

In KEGG analysis, the pathways of autophagy, FoxO, mTOR, MAPK and Ras signalling were highly enriched. Previously, studies have demonstrated that these pathways were closely associated with ECM (52,53). Dysregulation of autophagy under stress conditions plays a crucial role in progressive renal and hepatic fibrosis (54,55). The FoxO signalling pathway exerts key effects on renal fibrosis (56,57). Additionally, mTOR serves an essential role in cell proliferation and metabolism. The dysfunction of the mTOR pathway is involved in progression of renal fibrosis in various kidney diseases (58) and mediates fibrogenesis by regulating ECM accumulation (59). MAPK signalling is strongly active in ECM accumulation during the progression of DN (60). RAS effector RREB1 is considered to be a key partner of TGF- $\beta$ -activated SMAD transcription factors in ECM accumulation and epithelial-to-mesenchymal transitions (61). These results indicate that the differentially expressed tRFs may be associated with several signalling pathways and play important regulatory roles in the development of DN.

Finally, considering their potential pathophysiological mechanisms, the present study focused on downregulated tRFs. In particular, tRF-1:30-Gln-CTG-4 was further investigated since it was the most downregulated tRFs. Expression of tRF-1:30-Gln-CTG-4 decreased in the HG-treated group. ECM accumulation induced by HG treatment was reversed by the overexpression of tRF-1:30-Gln-CTG-4, which indicated that tRF-1:30-Gln-CTG-4 may have an antifibrotic role in DN progression. However, the mechanism by which tRF-1:30-Gln-CTG-4 regulates ECM secretion in DN remains unclear and warrants further investigation. Moreover, the effects of upregulated tRFs on HG-induced ECM accumulation were not investigated in the present study. Upregulated tRFs may also serve a critical role in promoting renal tubular injury and ECM accumulation. Thus, the exact effects of upregulated tRFs should be explored in a future study. It remains to be established whether the present results may also be observed in human kidney tissues.

In conclusion, the present study discovered that tRFs, which are novel types of sncRNAs, are associated with TIF

and involved in DN. The underlying mechanism may involve the dysregulation of autophagy and the FoxO, mTOR and MAPK signalling pathways. The present findings advance understanding of the pathophysiology of DN and may reveal promising therapeutic targets for the treatment of DN.

### Acknowledgements

Not applicable.

### Funding

The present study was supported by the National Natural Science Foundation of China (grant no. 81970664), Natural Science Foundation of Jiangsu Province (grants nos. BK20191082 and BK20211385) and 789 Outstanding Talent Program of SAHNMU (grants nos. 789ZYRC202080 119 and 789ZYRC202090251).

### Availability of data and materials

The datasets generated and/or analyzed during the current study are available in the Sequence Read Archive under BioProject repository, <https://www.ncbi.nlm.nih.gov/sra/PRJNA878883>.

### Authors' contributions

AZ and WG designed the study. JJ performed the experiments and wrote the manuscript. JR, HZ, HS, GQ and SL contributed to the data analysis. All authors have read and approved the final manuscript. JJ and AZ confirm the authenticity of all the raw data.

### Ethics approval and consent to participate

Animal experiments were approved by the Institutional Animal Care and Use Committee of Nanjing Medical University (approval no. 2206034). The human experimental procedures in the present study were approved by Nanjing Medical University [Nanjing, China; approval no. (2022)-KY-037-01] and written informed consent was obtained from all patients.

### Patient consent for publication

Not applicable.

### Competing interests

The authors declare that they have no competing interests.

### References

- Xue R, Gui D, Zheng L, Zhai R, Wang F and Wang N: Mechanistic insight and management of diabetic nephropathy: Recent progress and future perspective. *J Diabetes Res* 2017: 1839809, 2017.
- Tuttle KR, Jones CR, Daratha KB, Koyama AK, Nicholas SB, Alicic RZ, Duru OK, Neumiller JJ, Norris KC, Ríos Burrows N and Pavkov ME: Incidence of Chronic Kidney Disease among Adults with Diabetes, 2015-2020. *N Engl J Med* 387: 1430-1431, 2022.
- Alicic RZ, Rooney MT and Tuttle KR: Diabetic kidney disease: Challenges, progress and possibilities. *Clin J Am Soc Nephrol* 12: 2032-2045, 2017.
- Qi R and Yang C: Renal tubular epithelial cells: The neglected mediator of tubulointerstitial fibrosis after injury. *Cell Death Dis* 9: 1126, 2018.
- Huang F, Wang Q, Guo F, Zhao Y, Ji L, An T, Song Y, Liu Y, He Y and Qin G: FoxO1-mediated inhibition of STAT1 alleviates tubulointerstitial fibrosis and tubule apoptosis in diabetic kidney disease. *EBioMedicine* 48: 491-504, 2019.
- Pandey KK, Madhry D, Ravi Kumar YS, Malvankar S, Sapra L, Srivastava RK, Bhattacharyya S and Verma B: Regulatory roles of tRNA-derived RNA fragments in human pathophysiology. *Mol Ther Nucleic Acids* 26: 161-173, 2021.
- Fagan SG, Helm M and Prehn JHM: tRNA-derived fragments: A new class of non-coding RNA with key roles in nervous system function and dysfunction. *Prog Neurobiol* 205: 102118, 2021.
- Zeng TY, Hua YJ, Sun CX, Zhang Y, Yang F, Yang M, Yang Y, Li J, Huang X, Wu H, *et al*: Relationship between tRNA-derived fragments and human cancers. *Int J Cancer* 147: 3007-3018, 2020.
- Karaca E, Weitzer S, Pehlivan D, Shiraishi H, Gogakos T, Hanada T, Jhangiani SN, Wiszniewski W, Withers M, Campbell IM, *et al*: Human CLP1 mutations alter tRNA biogenesis, affecting both peripheral and central nervous system function. *Cell* 157: 636-650, 2014.
- Oberbauer V and Schaefer MR: tRNA-derived small RNAs: Biogenesis, modification, function and potential impact on human disease development. *Genes (Basel)* 9: 607, 2018.
- Khurana R, Ranches G, Schaffner S, Lukasser M, Rudnicki M, Mayer G and Hüttenhofer A: Identification of urinary exosomal noncoding RNAs as novel biomarkers in chronic kidney disease. *RNA* 23: 142-152, 2017.
- Shi H, Yu M, Wu Y, Cao Y, Li S, Qu G, Gong J, Gan W and Zhang A: tRNA-derived fragments (tRFs) contribute to podocyte differentiation. *Biochem Biophys Res Commun* 521: 1-8, 2020.
- Li S, Liu Y, He X, Luo X, Shi H, Qu G, Wen X, Gan W, Wang J and Zhang A: tRNA-Derived fragments in podocytes with Adriamycin-induced injury reveal the potential mechanism of idiopathic nephrotic syndrome. *Biomed Res Int* 2020: 7826763, 2020.
- Luo C, Zhou S, Zhou Z, Liu Y, Yang L, Liu J, Zhang Y, Li H, Liu Y, Hou FF and Zhou L: Wnt9a promotes renal fibrosis by accelerating cellular senescence in tubular epithelial cells. *J Am Soc Nephrol* 29: 1238-1256, 2018.
- Kilkenny C, Browne W, Cuthill IC, Emerson M and Altman DG; NC3Rs Reporting Guidelines Working Group: Animal Research: Reporting of in vivo experiments guidelines. *Br J Pharmacol* 160: 1577-1579, 2010.
- National Institutes of Health (NIH): Guide for the Care and Use of Laboratory Animals. In: National Research Council (US) Committee for the Update of the Guide for the Care and Use of Laboratory Animals. 7th Edition. National Academy Press, Washington, DC, 1996.
- Livak KJ and Schmittgen TD: Analysis of relative gene expression data using real-time quantitative PCR and the 2(-Delta Delta C(T)) Method. *Methods* 25: 402-408, 2001.
- Ji JL, Zhao YJ, Na C, Yang M, Zhu X, Shi H, Gan W and Zhang A: Connexin 43-autophagy loop in the podocyte injury of diabetic nephropathy. *Int J Mol Med* 44: 1781-1788, 2019.
- Peng F, Gong W, Li S, Yin B, Zhao C, Liu W, Chen X, Luo C, Huang Q, Chen T, *et al*: circRNA\_010383 Acts as a Sponge for miR-135a and its downregulated expression contributes to renal fibrosis in diabetic nephropathy. *Diabetes* 70: 603-615, 2021.
- Liu XQ, Jiang L, Lei L, Nie ZY, Zhu W, Wang S, Zeng HX, Zhang SQ, Zhang Q, Yard B and Wu YG: Carnosine alleviates diabetic nephropathy by targeting GNMT, a key enzyme mediating renal inflammation and fibrosis. *Clin Sci (Lond)* 134: 3175-3193, 2020.
- Wang XX, Wang D, Luo Y, Myakala K, Dobrinskikh E, Rosenberg AZ, Levi J, Kopp JB, Field A, Hill A, *et al*: FXR/TGR5 dual agonist prevents progression of nephropathy in diabetes and obesity. *J Am Soc Nephrol* 29: 118-137, 2018.
- Liu Y: Cellular and molecular mechanisms of renal fibrosis. *Nat Rev Nephrol* 7: 684-696, 2011.
- Yu X, Xie Y, Zhang S, Song X, Xiao B and Yan Z: tRNA-derived fragments: Mechanisms underlying their regulation of gene expression and potential applications as therapeutic targets in cancers and virus infections. *Theranostics* 11: 461-469, 2021.

24. Tuttle KR, Agarwal R, Alpers CE, Bakris GL, Brosius FC, Kolkhof P and Uribarri J: Molecular mechanisms and therapeutic targets for diabetic kidney disease. *Kidney Int* 102: 248-260, 2022.
25. Nellaiappan K, Preeti K, Khatri DK and Singh SB: Diabetic complications: An update on pathobiology and therapeutic strategies. *Curr Diabetes Rev* 18: e030821192146, 2022.
26. Xu Z, Zhang M, Wang Y, Chen R, Xu S, Sun X, Yang Y, Lin Z, Wang S and Huang H: Gentiopicroside ameliorates diabetic renal tubulointerstitial fibrosis via inhibiting the AT1R/CK2/NF- $\kappa$ B pathway. *Front Pharmacol* 13: 848915, 2022.
27. Martens-Uzunova ES, Olvedy M and Jenster G: Beyond microRNA-novel RNAs derived from small non-coding RNA and their implication in cancer. *Cancer Lett* 340: 201-211, 2013.
28. Wang Y, Weng Q, Ge J, Zhang X, Guo J and Ye G: tRNA-derived small RNAs: Mechanisms and potential roles in cancers. *Genes Dis* 9: 1431-1442, 2022.
29. George S, Rafi M, Aldarmaki M, ElSiddig M, Al Nuaimi M and Amiri KMA: tRNA derived small RNAs-Small players with big roles. *Front Genet* 13: 997780, 2022.
30. Lu Z, Su K, Wang X, Zhang M, Ma S, Li H and Qiu Y: Expression profiles of tRNA-derived small rnas and their potential roles in primary nasopharyngeal carcinoma. *Front Mol Biosci* 8: 780621, 2021.
31. Li S, Xu Z and Sheng J: tRNA-derived small RNA: A novel regulatory small non-coding RNA. *Genes (Basel)* 9: 246, 2018.
32. Yu M, Lu B, Zhang J, Ding J, Liu P and Lu Y: tRNA-derived RNA fragments in cancer: Current status and future perspectives. *J Hematol Oncol* 13: 121, 2020.
33. Guzzi N and Bellodi C: Novel insights into the emerging roles of tRNA-derived fragments in mammalian development. *RNA Biol* 17: 1214-1222, 2020.
34. Zhang Y, Bi Z, Dong X, Yu M, Wang K, Song X, Xie L and Song X: tRNA-derived fragments: tRF-Gly-CCC-046, tRF-Tyr-GTA-010 and tRF-Pro-TGG-001 as novel diagnostic biomarkers for breast cancer. *Thorac Cancer* 12: 2314-2323, 2021.
35. Li D, Zhang H, Wu X, Dai Q, Tang S, Liu Y, Yang S and Zhang W: Role of tRNA derived fragments in renal ischemia-reperfusion injury. *Ren Fail* 44: 815-825, 2022.
36. Lee YS, Shibata Y, Malhotra A and Dutta A: A novel class of small RNAs: tRNA-derived RNA fragments (tRFs). *Genes Dev* 23: 2639-2649, 2009.
37. Pan Q, Han T and Li G: Novel insights into the roles of tRNA-derived small RNAs. *RNA Biol* 18: 2157-2167, 2021.
38. Soares AR and Santos M: Discovery and function of transfer RNA-derived fragments and their role in disease. *Wiley Interdiscip Rev RNA* 8: e1423, 2017.
39. Zhu P, Lu J, Zhi X, Zhou Y, Wang X, Wang C, Gao Y, Zhang X, Yu J, Sun Y and Zhou P: tRNA-derived fragment tRFLys-CTT-010 promotes triple-negative breast cancer progression by regulating glucose metabolism via G6PC. *Carcinogenesis* 42: 1196-1207, 2021.
40. Zhong F, Hu Z, Jiang K, Lei B, Wu Z, Yuan G, Luo H, Dong C, Tang B, Zheng C, *et al.*: Complement C3 activation regulates the production of tRNA-derived fragments Gly-tRFs and promotes alcohol-induced liver injury and steatosis. *Cell Res* 29: 548-561, 2019.
41. Haussecker D, Huang Y, Lau A, Parameswaran P, Fire AZ and Kay MA: Human tRNA-derived small RNAs in the global regulation of RNA silencing. *RNA* 16: 673-695, 2010.
42. Shen Y, Yu X, Zhu L, Li T, Yan Z and Guo J: Transfer RNA-derived fragments and tRNA halves: Biogenesis, biological functions and their roles in diseases. *J Mol Med (Berl)* 96: 1167-1176, 2018.
43. Han Y, Peng Y, Liu S, Wang X, Cai C, Guo C, Chen Y, Gao L, Huang Q, He M, *et al.*: tRF3008A suppresses the progression and metastasis of colorectal cancer by destabilizing FOXK1 in an AGO-dependent manner. *J Exp Clin Cancer Res* 41: 32, 2022.
44. Goodarzi H, Liu X, Nguyen HC, Zhang S, Fish L and Tavazoie SF: Endogenous tRNA-derived fragments suppress breast cancer progression via YBX1 displacement. *Cell* 161: 790-802, 2015.
45. Fabregat I, Moreno-Caceres J, Sanchez A, Dooley S, Dewidar B, Giannelli G and Ten Dijke P: IT-LIVER Consortium: TGF- $\beta$  signaling and liver disease. *FEBS J* 283: 2219-2232, 2016.
46. Lear TB, Lockwood KC, Larsen M, Tuncer F, Kennerdell JR, Morse C, Valenzi E, Tabib T, Jurczak MJ, Kass DJ, *et al.*: Kelch-like protein 42 is a profibrotic ubiquitin E3 ligase involved in systemic sclerosis. *J Biol Chem* 295: 4171-4180, 2020.
47. Li L, Kang H, Zhang Q, D'Agati VD, Al-Awqati Q and Lin F: FoxO3 activation in hypoxic tubules prevents chronic kidney disease. *J Clin Invest* 129: 2374-2389, 2019.
48. Herman-Edelstein M, Scherzer P, Tobar A, Levi M and Gafter U: Altered renal lipid metabolism and renal lipid accumulation in human diabetic nephropathy. *J Lipid Res* 55: 561-572, 2014.
49. Wang W, Luo Y, Yang S, Zeng M, Zhang S, Liu J, Han Y, Liu Y, Zhu X, Wu H, *et al.*: Ectopic lipid accumulation: Potential role in tubular injury and inflammation in diabetic kidney disease. *Clin Sci (Lond)* 132: 2407-2422, 2018.
50. Chen X, Han Y, Gao P, Yang M, Xiao L, Xiong X, Zhao H, Tang C, Chen G, Zhu X, *et al.*: Disulfide-bond A oxidoreductase-like protein protects against ectopic fat deposition and lipid-related kidney damage in diabetic nephropathy. *Kidney Int* 95: 880-895, 2019.
51. Falconi M, Giangrossi M, Zabaleta ME, Wang J, Gambini V, Tilio M, Bencardino D, Occhipinti S, Belletti B, Laudadio E, *et al.*: A novel 3'-tRNA<sup>Glu</sup>-derived fragment acts as a tumor suppressor in breast cancer by targeting nucleolin. *FASEB J* 33: 13228-13240, 2019.
52. Livingston MJ, Shu S, Fan Y, Li Z, Jiao Q, Yin XM, Venkatachalam MA and Dong Z: Tubular cells produce FGF2 via autophagy after acute kidney injury leading to fibroblast activation and renal fibrosis. *Autophagy* 1-22, 2022 (Epub ahead of print).
53. Majumder S, Ren L, Pushpakumar S and Sen U: Hydrogen sulphide mitigates homocysteine-induced apoptosis and matrix remodelling in mesangial cells through Akt/FOXO1 signalling cascade. *Cell Signal* 61: 66-77, 2019.
54. Tang C, Han H, Yan M, Zhu S, Liu J, Liu Z, He L, Tan J, Liu Y, Liu H, *et al.*: PINK1-PRKN/PARK2 pathway of mitophagy is activated to protect against renal ischemia-reperfusion injury. *Autophagy* 14: 880-897, 2018.
55. Kong D, Zhang Z, Chen L, Huang W, Zhang F, Wang L, Wang Y, Cao P and Zheng S: Curcumin blunts epithelial-mesenchymal transition of hepatocytes to alleviate hepatic fibrosis through regulating oxidative stress and autophagy. *Redox Biol* 36: 101600, 2020.
56. Rao P, Qiao X, Hua W, Hu M, Tahan M, Chen T, Yu H, Ren X, Cao Q, Wang Y, *et al.*: Promotion of  $\beta$ -catenin/forkhead box protein O signaling mediates epithelial repair in kidney injury. *Am J Pathol* 191: 993-1009, 2021.
57. Qiao X, Rao P, Zhang Y, Liu L, Pang M, Wang H, Hu M, Tian X, Zhang J, Zhao Y, *et al.*: Redirecting TGF- $\beta$  Signaling through the  $\beta$ -Catenin/Foxo complex prevents kidney fibrosis. *J Am Soc Nephrol* 29: 557-570, 2018.
58. Ma MKM, Yung S and Chan TM: mTOR inhibition and kidney diseases. *Transplantation* 102 (2S Suppl 1): S32-S40, 2018.
59. Jimenez-Urbe AP, Gomez-Sierra T, Aparicio-Trejo OE, Orozco-Ibarra M and Pedraza-Chaverri J: Backstage players of fibrosis: NOX4, mTOR, HDAC and S1P; companions of TGF- $\beta$ . *Cell Signal* 87: 110123, 2021.
60. Malik S, Suchal K, Khan SI, Bhatia J, Kishore K, Dinda AK and Arya DS: Apigenin ameliorates streptozotocin-induced diabetic nephropathy in rats via MAPK-NF- $\kappa$ B-TNF- $\alpha$  and TGF- $\beta$ 1-MAPK-fibronectin pathways. *Am J Physiol Renal Physiol* 313: F414-F422, 2017.
61. Su J, Morgani SM, David CJ, Wang Q, Er EE, Huang YH, Basnet H, Zou Y, Shu W, Soni RK, *et al.*: TGF- $\beta$  orchestrates fibrogenic and developmental EMTs via the RAS effector RREB1. *Nature* 577: 566-571, 2020.



This work is licensed under a Creative Commons Attribution-NonCommercial-NoDerivatives 4.0 International (CC BY-NC-ND 4.0) License.